

Complete neutron-multiplicity distributions in fast-neutron-induced fission

B. Fraïsse ^{*}, G. Bélier , V. Méot , L. Gaudefroy , A. Francheteau , and O. Roig
CEA DAM DIF, F-91297 Arpajon, France and Université Paris-Saclay, LMCE, 91680 Bruyères-le-Châtel, France



(Received 29 March 2023; accepted 15 June 2023; published 19 July 2023)

The average number of neutrons emitted in neutron-induced nuclear fission has been measured for major actinides from thermal to relativistic incident energy ranges. On the other hand, the complete probability distributions could not be reconstructed from experimental data beyond a few MeV because the unfolding of the neutron-counter response is an ill-conditioned inverse problem. In order to obtain the complete neutron-multiplicity distributions without simplifying assumption on their shapes, this paper submits a robust Tikhonov-inspired regularization procedure. A reevaluation, with this method, of the only available dataset, provides precise neutron-multiplicity distributions for uranium-235 and plutonium-239 up to 12 MeV. Their exact shapes are exploited to extract, for the first time from experimental data, the second-chance fission partial probability.

DOI: [10.1103/PhysRevC.108.014610](https://doi.org/10.1103/PhysRevC.108.014610)

I. INTRODUCTION

The number of prompt neutrons produced by nuclear fission plays a foremost role in society, e.g., in low-carbon energy production or nonproliferation. While the average neutron multiplicity $\bar{\nu}$ was sufficient for many applications, an increasing number of problems require the knowledge of complete distributions $P(\nu)$. For example, in reactor physics, ultrarealistic Monte Carlo simulations using complete $P(\nu)$ could provide a better understanding of low-power phenomena such as clustering [1]. In nuclear safeguards, since $\bar{\nu}$ values are close for most actinides, the isotopic composition of a sample is inferred from the neutron-multiplicity moments [2,3]. Reliable $P(\nu)$ at any incident neutron energy would increase the accuracy of nondestructive assay techniques.

The neutron-multiplicity distributions also offer an insight into the complex dynamics of the fission process. Based on the Hauser-Feshbach theory, recent computational works reported an intimate connection between the neutron-multiplicity-distribution shape and the fission-fragment spin distribution [4,5].

However, the neutron-multiplicity moments beyond the average value suffer from a lack of measurements in the fast-neutron regime. This paper diagnoses how ill conditioning of the neutron-counter response matrix was the main obstacle for the unfolding of complete neutron-multiplicity distributions. A robust method is submitted to overcome this difficulty and applied to Fréhaut's measurements [6]. As far as we know, it is the only fission neutron counting beyond the second-chance threshold. The complete $P(\nu)$ are finally exploited to extract, for the first time from experimental data, the second-chance partial probability. These results could be utilized for constraining evaluated data: $P(\nu)$ have recently been included

into ENDF and multichance fission physics incorporates many parameters like fission barriers, neutron transmission coefficients, and nuclear level densities.

II. STATE OF THE ART

Since the pioneering studies in the 1950s, the average number of neutrons released in nuclear fission has been measured for a wide variety of actinides and incident energy ranges including spontaneous fission [7–10], photofission [11], thermal-neutron-induced fission [12–15], and fast-neutron-induced fission from a few MeV [13,14,16,17] to tens of MeV [18,19]. The true average neutron multiplicity is deduced from its measurement $\bar{\nu}_{\text{exp}}$ and the detection efficiency ε as

$$\bar{\nu} = \frac{\bar{\nu}_{\text{exp}}}{\varepsilon}. \quad (1)$$

Nuclear fission, though, is a complex process where fragment splitting, kinetic energy, deformation, and excitation energy are all varying quantities. Therefore, the neutron multiplicity is distributed and the shape of this distribution integrates all these fluctuations.

On the one hand, a generalization of Eq. (1) makes it possible to derive an approximation of any moment [20] from the k th order factorial moments of the experimental distribution f_k^{exp} and the Stirling numbers of the second kind, like the standard deviation

$$\sigma \approx \sqrt{\sum_{j=0}^2 \left\{ \begin{matrix} 2 \\ j \end{matrix} \right\} \frac{f_j^{\text{exp}}}{\varepsilon^j} - \bar{\nu}^2}. \quad (2)$$

Nonetheless, such a procedure is highly unstable: the error on each moment is transferred to the next one and excessively amplified by a power law.

On the other hand, the unfolding of the complete distribution $P(\nu)$ must take into account that the emission of n

^{*}baptiste.fraisse@cea.fr

neutrons can lead to the counting of n , $n - 1$, $n - 2$, or less neutrons. Such a detection process is naturally modeled by a random binomial sampling. Let $\mathbf{X} \in \mathbb{R}^{n_{\max}}$ be the vector of true neutron-multiplicity distribution cut at some maximum value n_{\max} and $\mathbf{Y} \in \mathbb{R}^{n_{\max}}$ its measurement. The detection efficiency unfolding takes the form of a linear inverse problem $\mathbf{Y} = \mathbb{A}\mathbf{X}$ with

$$[\mathbb{A}]_{nm} = \begin{cases} \binom{m}{n} \varepsilon^n (1 - \varepsilon)^{m-n} & \text{if } n \leq m \\ 0 & \text{else.} \end{cases} \quad (3)$$

The detection operator $\mathbb{A} \in \mathbb{R}^{n_{\max} \times n_{\max}}$ is upper triangular—there are no more detected than emitted neutrons after noise subtraction—and it is invertible. Since Diven's works in the 1950s [7], the neutron-multiplicity distributions are usually unfolded by a direct inversion method $\mathbf{X} = \mathbb{A}^{-1}\mathbf{Y}$ with

$$[\mathbb{A}^{-1}]_{nm} = \begin{cases} \binom{m}{n} \varepsilon^{-m} (\varepsilon - 1)^{m-n} & \text{if } n \leq m \\ 0 & \text{else.} \end{cases} \quad (4)$$

The direct inversion method described by Eq. (4) has been used to unfold neutron-multiplicity distributions for spontaneous fission [8,21], photofission [22], and thermal-neutron-induced fission [7,12,15].

In contrast, there are no such directly unfolded distributions for fast neutrons. The direct inversion method was indeed reported to return unstable and unphysical distributions [2,23–25]. Mathematically speaking, the inverse problem (3) is the discretized version of a Fredholm integral and more specifically a Volterra integral since \mathbb{A} is triangular like time-dependent problems due to the causal principle. This class of inverse problems is commonly ill conditioned in the sense of Hadamard [26]: if \mathbb{A} is invertible, the condition number $\text{cond}(\mathbb{A})$ for the Frobenius norm is such that $\text{cond}(\mathbb{A}) := \|\mathbb{A}\| \times \|\mathbb{A}^{-1}\| \gg 1$. If so, the direct inversion method can lead to an unphysical distribution \mathbf{X} because the condition number scales the propagation $\delta\mathbf{X}$ of the experimental errors $\delta\mathbf{Y}$ [27] like

$$\frac{\|\delta\mathbf{X}\|}{\|\mathbf{X}\|} \leq \text{cond}(\mathbb{A}) \frac{\|\delta\mathbf{Y}\|}{\|\mathbf{Y}\|}. \quad (5)$$

The condition number versus the maximum neutron multiplicity to consider n_{\max} in Fig. 1 reveals the reason why multiplicity distributions were not unfolded for fast-neutron-induced fissions: they need to be described by large n_{\max} of typically 10 and thus large condition numbers. Thermal-neutron-induced fissions are properly described by small n_{\max} of typically 6 and thus smaller condition numbers for the same detection efficiency. Therefore, the direct unfolding method (4) is unfeasible for fast neutrons unless a very large statistics is available. In order to bypass this difficulty, least-squares regressions of predefined shapes for $P(\nu)$ were attempted in the literature using polynomial [28,29], Gaussian [8], and skew-Gaussian distributions [2,23]. Yet, no study supports that $P(\nu)$ remains such a basic function for fast neutrons. There is even evidence that skew-Gaussian distributions lead to unphysical discontinuities from one incident energy to another [2].

Recent works successfully initiate the use of regularization tools for the unfolding of $P(\nu)$ in superheavy nuclei spontaneous fission [30–32]. To make such methods robust

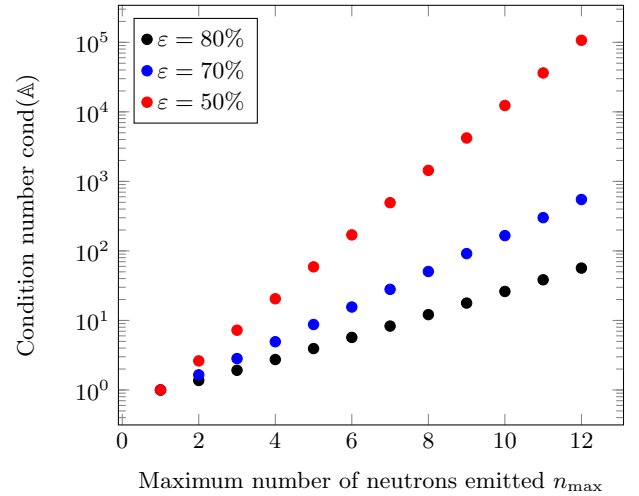


FIG. 1. Condition number of the neutron-counter response matrix vs the maximum number of neutrons to consider. Three detection efficiencies are presented.

enough for the systematic unfolding of $P(\nu)$ in fast-neutron-induced fission, we had to reinforce them with the addition of a non-negativity constraint and a formal criterion for the regularization parameter choice.

III. METHOD

This section presents a robust Tikhonov regularization procedure in order to generalize Diven's method from Eq. (4) for the unfolding of neutron-multiplicity distributions in fast-neutron-induced fission.

A. Formalism

The regularization procedure aims to get a physical solution from the generalized inverse problem [33,34]:

$$\text{Find } \mathbf{X} \in \mathbb{R}^{n_{\max}} \text{ such as } \min \|\mathbb{A}\mathbf{X} - \mathbf{Y}\|. \quad (6)$$

Let \mathbb{D} be the matrix representation of regularity requirements for \mathbf{X} in order to be physically acceptable. In the case of neutron multiplicity, \mathbb{D} merely encodes the second derivative and vanishing conditions out of the multiplicity domain. A physically acceptable solution of Eq. (6) must verify, for a chosen $\eta \in \mathbb{R}$,

$$\begin{aligned} &\text{Find } \tilde{\mathbf{X}}_{\eta} \in \mathbb{R}^{n_{\max}} \\ &\text{such as } \min \|\mathbb{A}\tilde{\mathbf{X}}_{\eta} - \mathbf{Y}\| \\ &\text{subject to } \|\mathbb{D}\tilde{\mathbf{X}}_{\eta}\| \leq \eta \\ &\text{and } \tilde{\mathbf{X}}_{\eta} \geq 0. \end{aligned} \quad (7)$$

The Tikhonov regularization is the set of problems obtained from the Kuhn-Tucker conditions

$$\begin{aligned} &\text{Find } \tilde{\mathbf{X}}_{\lambda} \in \mathbb{R}^{n_{\max}} \\ &\text{such as } \min(\|\mathbb{A}\tilde{\mathbf{X}}_{\lambda} - \mathbf{Y}\| + \lambda \|\mathbb{D}\tilde{\mathbf{X}}_{\lambda}\|) \\ &\text{subject to } \tilde{\mathbf{X}}_{\lambda} \geq 0. \end{aligned} \quad (8)$$

The Lagrange multiplier $\lambda \in \mathbb{R}^+$ is called the *regularization parameter*. The regularization procedure can be interpreted as a spectral high-pass filter and the regularization parameter λ is related to its cutoff. This property can be noticed on the normal equation

$$(\mathbb{A}^\top \mathbb{A} + \lambda^2 \mathbb{D}^\top \mathbb{D}) \tilde{\mathbf{X}}_\lambda = \mathbb{A}^\top \mathbf{Y}. \quad (9)$$

Projected on the basis $(\mathbf{u}_i, \mathbf{v}_i)$ from the generalized singular value decomposition [35] of the couple (\mathbb{A}, \mathbb{D}) associated with the singular values (a_i, d_i) , the normal equation gives

$$\tilde{\mathbf{X}}_\lambda = \sum_{i=1}^{n_{\max}} \phi_i(\mathbf{Y}, \mathbf{u}_i) \mathbf{v}_i, \quad \text{with} \quad \phi_i = \frac{a_i}{a_i^2 + \lambda^2 d_i^2}. \quad (10)$$

Filter coefficients ϕ_i appear: they vanish if $a_i^2 \ll \lambda^2 d_i^2$ but take part as $\phi_i \rightarrow 1/a_i$ otherwise [27]. The propagation of uncertainties can also be analytically derived [36] with $\mathbb{B} = (\mathbb{A}^\top \mathbb{A} + \lambda^2 \mathbb{D}^\top \mathbb{D}) \mathbb{A}^\top$ as

$$\text{cov}(\tilde{\mathbf{X}}_\lambda) = \mathbb{B} \text{cov}(\mathbf{Y}) \mathbb{B}^\top. \quad (11)$$

The selection of the optimum parameter λ^* , resulting from a balance between accuracy and smoothing strength, is crucial for the regularization procedure success and bias inhibition. For the unfolding of neutron-multiplicity distributions in superheavy nuclei spontaneous fission, recent works [31,32] used a ‘‘physical’’ criterion: the reconstructed distribution must match with the expected mean value from Eq. (1) and standard deviation approximation from Eq. (2). However, this criterion may become equivocal in practice: several regularization parameters can deliver a satisfying matching with low-order moments while the distribution as a whole is wrong. Therefore, the present paper focuses on two criteria developed in the framework of applied mathematics [27,36,37]. The first one, the \mathcal{L} -curve method, studies the phase transition from over-regularized to under-regularized distributions through the tradeoff curve:

$$\mathcal{L}(\lambda) : (\|\mathbf{Y} - \mathbb{A} \tilde{\mathbf{X}}_\lambda\|, \|\mathbb{D} \tilde{\mathbf{X}}_\lambda\|). \quad (12)$$

The optimum parameter is found at the critical point, identified at the maximum curvature:

$$\lambda_{\mathcal{L}}^* : \max_{\lambda \in \mathbb{R}^+} \left\{ \mathcal{C}(\lambda) = \frac{\mathcal{L}''(\lambda)}{[1 + \mathcal{L}'(\lambda)^2]^{\frac{3}{2}}} \right\}. \quad (13)$$

Since the finite difference estimation of curvature in Eq. (13) is a source of error, the critical point will be rather picked out at the farthest point orthogonally projected onto the segment connecting the two ends of the \mathcal{L} curve. The second criterion we consider is the generalized cross validation (GCV) given by

$$\lambda_{\text{GCV}}^* : \min_{\lambda \in \mathbb{R}^+} \left\{ \text{GCV}(\lambda) = \frac{\|\mathbf{Y} - \mathbb{A} \tilde{\mathbf{X}}_\lambda\|}{(n_{\max} - 1) - \sum_i \phi_i(\lambda)} \right\}. \quad (14)$$

B. Validation

As a proof of concept, the regularization procedure described by Eq. (8) is applied on sampled representative

functions submitted to the detection operator. Detailed in Table I, different data entries are studied in order to investigate typical detection efficiencies ε and numbers of fission events \mathcal{N}_f as well as distributions distorted by a skewness β or a kurtosis κ . The validation criteria are the relative errors on the average value $\Delta \bar{\nu}$, standard deviation $\Delta \sigma$, skewness $\Delta \beta$, kurtosis $\Delta \kappa$, and the Euclidean distance d from the whole distribution. The \mathcal{L} -curve and GCV methods could separately underestimate or overestimate the regularization parameter. In practice, such marginal variations do not change significantly $P(\nu)$ but, for sturdiness, λ^* is taken as the average of λ_{GCV}^* and $\lambda_{\mathcal{L}}^*$.

Qualitatively, Fig. 2 illustrates the success of the regularization procedure (green histogram) reproducing accurately the sampled distribution (black curve) from the measured one (red histogram) while the direct inversion (gray histogram) is wrong. Quantitatively, Table I demonstrates the capability of the regularization procedure to return accurate data for usual conditions (E1, E3, E5, and E6). The regularization procedure is reaching its limits for low efficiency (E2) or poor statistics (E4).

IV. REVALUATION OF FRÉHAUT'S DATA

In this section, the regularization method is applied on Fréhaut's neutron counting dataset [6]. It went back and forth between different groups [24,25,28], trying to unfold the complete distributions, and it was finally decided to assume the shape of the distributions as third-order polynomials or Gaussian distributions versus the incident neutron energy. Discussing these assumptions, it was specified that the unfolding instabilities ‘‘could be in principle removed using the *a priori* information we have on the smoothness of the distribution but the corresponding mathematical formalism remains to be developed’’ [24]. The procedure from Sec. II is

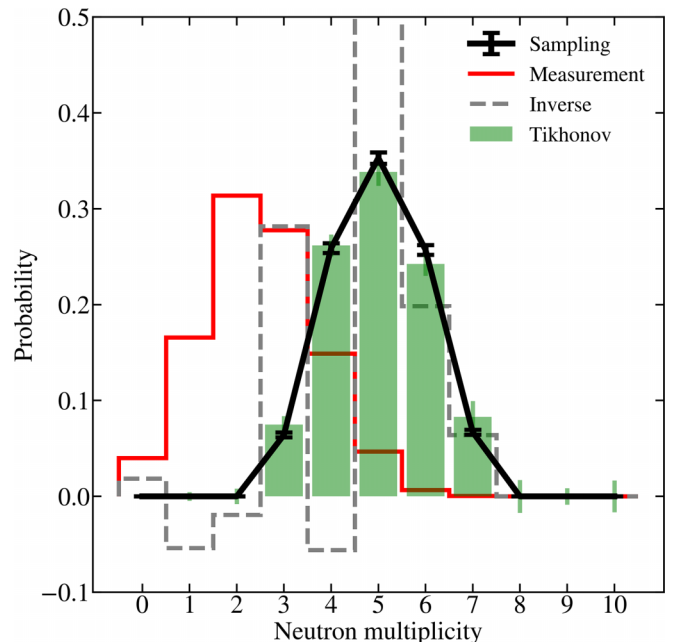


FIG. 2. Tikhonov regularization for the case E6 from Table I.

TABLE I. Case studies for the validation of the regularization procedure described by Eq. (8). See the text for notations. Typical experimental values are explored for detection efficiency ε , number of fission events \mathcal{N}_f , and the neutron-multiplicity moments: $\bar{\nu}$, σ , β , and κ .

Case study	Distribution	ε (%)	\mathcal{N}_f	$\bar{\nu}$	σ	β	κ	λ_{GCV}^*	$\lambda_{\mathcal{L}}^*$	$\Delta\bar{\nu}$ (%)	$\Delta\sigma$	$\Delta\beta$ (%)	$\Delta\kappa$ (%)	d (%)
E1	Gaussian	50	10^4	5.0	1.0	0	0	0.008	0.011	0	3			7
E2	Gaussian	25	10^4	5.0	1.0	0	0	0.013	0.003	1	8			8
E3	Gaussian	80	10^4	5.0	1.0	0	0	0.029	0.342	1	8			8
E4	Gaussian	50	10^3	5.0	1.0	0	0	0.033	0.063	1	10			7
E5	Skew-Gaussian	50	10^4	5.0	1.0	0.1	0	0.013	0.018	2	2	6		5
E6	Raised cosine	50	10^4	5.0	1.0	0	-0.6	0.062	0.020	0	3		8	5

taken for this formalism. The reevaluation of this dataset is an opportunity as Fréhaut's neutron counter was highly efficient ($\varepsilon \approx 83\%$ measured with a californium-252 source) and lies behind many modern evaluations. For conciseness, the discussion will focus on uranium-235 but the same treatments are carried out for plutonium-239. Uranium-238 data are not exploitable because of the poor statistics close to the E4 case in Table I.

The complete neutron-multiplicity distributions $P(\nu)$ unfolded by the regularization procedure are given in the Appendix. We emphasize that, for the first time, no assumption on their shapes was made and no unphysical discontinuities show up from one incident energy to another. Additionally, it is checked in Fig. 3 that $\bar{\nu}$ values derived from those regularized distributions are in excellent agreement with the ENDF-BVIII evaluation.

The standard deviations, formerly unpublished due to their extreme sensitivity to the unfolding instabilities, are derived from the regularized distributions in Fig. 4. Below the second-chance threshold, they exhibit an approximately linear increasing trend. For uranium-235, the slope is $0.011 \pm$

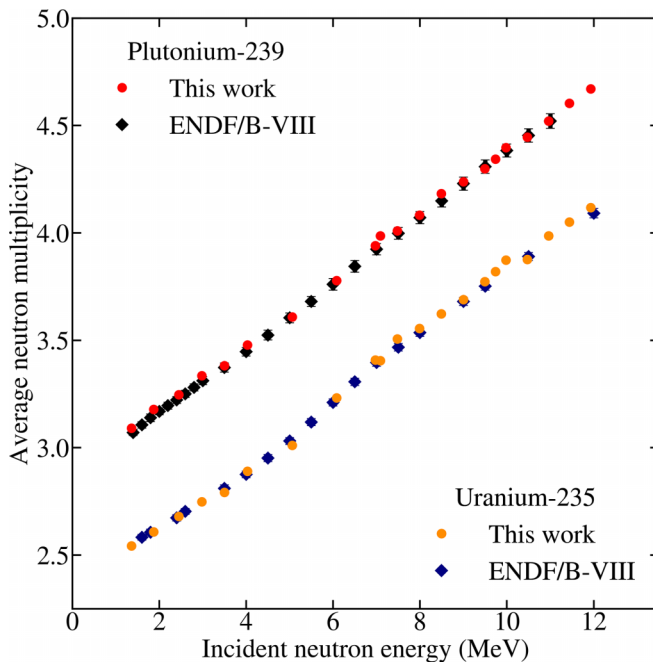


FIG. 3. Average neutron multiplicity $\bar{\nu}$ from regularized $P(\nu)$. Error bars (not visible) come from Eq. (11).

0.002 MeV^{-1} with a coefficient of determination $R^2 = 0.88$ and the intercept of 1.10 ± 0.02 is consistent with the value for thermal neutrons of 1.07 ± 0.02 [7,38]. For plutonium-239, the slope is $0.011 \pm 0.003 \text{ MeV}^{-1}$ with $R^2 = 0.68$ and the intercept of 1.14 ± 0.02 is consistent with the value for thermal neutrons of 1.14 ± 0.07 [7,38].

The surprising “universality” of the standard deviation values around 1.1, reported in the literature in spontaneous and thermal-neutron-induced fission for most actinides [7,38,39], seems to generalize as a similar linear law for fast neutrons. The coefficients of determination suffer from the uncontrolled systematic errors of this dataset. We understand these fluctuations as coming from corrections made because of different sources. For instance, the points at 6.97 and 7.09 MeV, respectively, from $d-d$ and $p-t$ sources, have a spurious gap.

In addition, the standard deviation clearly exhibits a local minimum around the first- to second-chance fission transition. As far as we know, this behavior is captured only

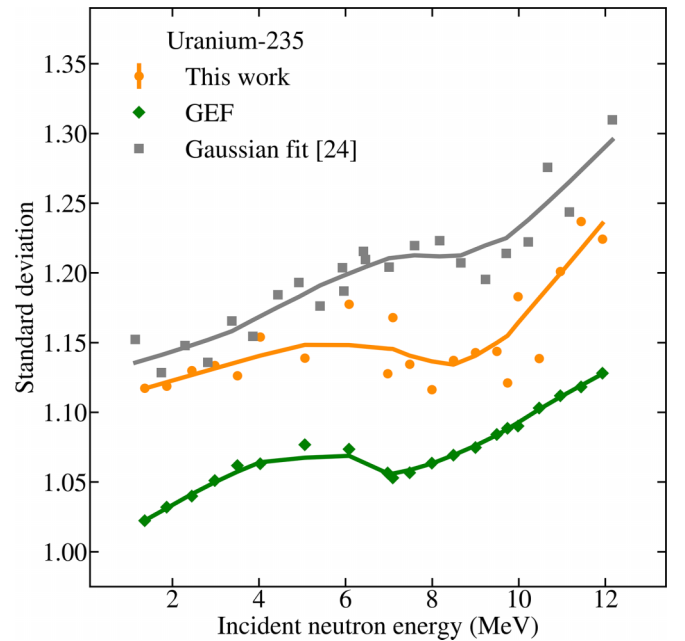


FIG. 4. Neutron-multiplicity standard deviation σ . Error bars come from Eq. (11). Below the second-chance fission threshold $\sigma \approx 0.011 \times E_n + 1.10$ with $R^2 = 0.88$. The gray squares result from a Gaussian fit unfolding method [24]. Solid lines are running averages to guide the eye.

by the GEF code [40] despite a systematic underestimation. Unlike Tikhonov regularization, the unfolding methods based on simple shapes for $P(\nu)$ essentially remove this structure. For example, the gray squares in Fig. 4 are extracted from Gaussian fits [24].

The local drop in standard deviation can be explained by two concurrent mechanisms. The first one, due to the second-chance fission channel opening, is the deterministic emission of a prefission neutron. The multiplicity fluctuation is consequently locally deflected. The second one results from the intimate mixture of neutron-multiplicity distributions $p_1(\nu)$ and $p_2(\nu)$ from first- and second-chance fission, respectively. This is written

$$P(\nu) = (1 - x) p_1(\nu) + x p_2(\nu), \quad (15)$$

where the mixing ratio x is the second-chance probability. As seen previously, the standard deviation is roughly linear with incident energy below the second-chance threshold. Assuming that this behavior is approximately preserved beyond but in the space of excitation energy, the second-chance fissioning system having a lower excitation energy than $p_2(\nu)$ is narrower than $p_1(\nu)$. Therefore, $P(\nu)$ becomes locally narrower before $p_2(\nu)$ gets wider in turn.

The neutron-multiplicity mixture described by Eq. (15) can be solved to find the second-chance probability. To do this, realistic models for $p_1(\nu)$ and $p_2(\nu)$ are required. Below the second-chance threshold, neutron-multiplicity distributions are precisely described by raised cosine distributions $\mathcal{R}[\bar{\nu}, \sigma]$. This observation differs slightly from the Gaussian distribution usually reported in the literature for spontaneous or thermal-neutron-induced fission. This is due to a small kurtosis close to -0.5 for every energy in the $P(\nu)$ unfolded by the Tikhonov regularization. The average neutron multiplicity and standard deviation, approximately linear with incident energy before the second-chance threshold, are assumed linear with excitation energy up to 12 MeV. This assumption extends the linear relationship observed before the second-chance threshold to a few more MeV. Under this hypothesis, the neutron-multiplicity distribution $i \in \{1, 2\}$ is modeled as follows:

$$p_i(\nu) \approx \mathcal{R}[\bar{\nu} = a_i \bar{E}_i + b_i, \sigma = c_i \bar{E}_i + d_i](\nu - \delta_{i,2}). \quad (16)$$

The Kronecker delta $\delta_{i,2}$ is the prefission neutron shift. The “equivalent” incident energy for the first-chance fission is simply the incident neutron energy $\bar{E}_1 = E_n$. The “equivalent” incident neutron energy for second-chance fission is generalized as the excitation energy of the fissioning nucleus E_i subtracted from its neutron separation energy S_n and the average prefission neutron energy \bar{E}'_n such as $\bar{E}_2 = E_2 - S_n - \bar{E}'_n$. The excitation energy is given by the incident neutron energy increased by the neutron separation energy of the compound nucleus $E_2 = E_n + S_n$. The neutron separation energies are taken from Los Alamos National Laboratory public data [41] and the average prefission neutron energies from GEF. The parameters a_1 , b_1 , c_1 , and d_1 are taken from the linear fit of experimental quantities $\bar{\nu}$ and σ below the second-chance fission threshold. The parameters a_2 and b_2 come from the ENDF-BVIII evaluation of $\bar{\nu}$ for uranium-234. The parameters c_2 and d_2 rule the standard deviation for uranium-234: there

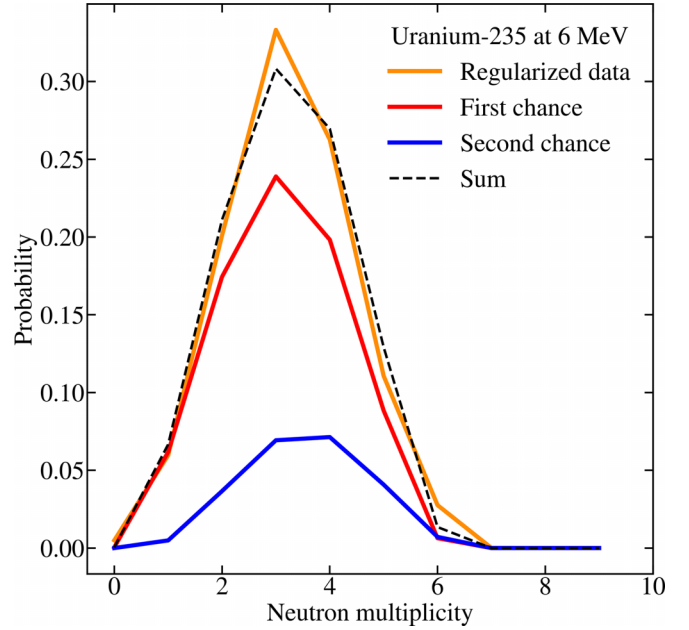


FIG. 5. Fit from Eq. (15) for uranium-235 at 6 MeV. A mixture (black dashed line) of p_1 (red solid line) and p_2 (blue solid line) is required to minimize the χ^2 distance from the neutron-multiplicity distribution unfolded from experimental data by the regularization procedure (orange solid line).

are no such data in the literature but, as previously discussed, similar values are expected for close-in-mass nuclei. For the needs of the model, these parameters are thus taken identical to uranium-235 ones, i.e., $c_2 = c_1$ and $d_2 = d_1$. The parameters are summarized in Table II. The mixing ratio x is finally obtained as the minimizer of χ^2 distance between Eq. (15) and the regularized distributions.

A critical fit at 6 MeV is displayed in Fig. 5, during the first- to second-chance transition, where $P(\nu)$ requires a mixture of $p_1(\nu)$ and $p_2(\nu)$ to be accurately fitted. Additionally, the average neutron multiplicity was checked to be perfectly reproduced by these fits.

The mixing ratio x for each incident neutron energy is plotted in Fig. 6 for uranium-235 and plutonium-239. This result is an indirect but first measurement of the second-chance fission partial probability. It is deeply rooted in the clues left by the multichance competition in the $P(\nu)$ shapes—especially the standard deviation—precisely unfolded by the Tikhonov regularization. The error bars are estimated as the quadratic sum of statistical errors from Eq. (11) and arbitrary $\pm 10\%$ over the experimentally unknown parameter \bar{E}'_n . For uranium-235, our plateau lies between GEF, ENDF-BVII, and HF3D [5]. For plutonium-239, our result indicates a continuously growing trend also predicted by GEF and ENDF-BVII.

V. DISCUSSION

The extraction of the second-chance partial probability was made under the assumption of similar standard deviation laws for close-in-mass nuclei. This property is supported by all existing measurements for thermal neutrons

TABLE II. Parameters for the neutron-multiplicity-distribution mixture in Eq. (16). See the text for notations.

Nucleus	S_n (MeV)	a_1 (MeV $^{-1}$)	b_1	c_1 (MeV $^{-1}$)	d_1	a_2 (MeV $^{-1}$)	b_2	c_2 (MeV $^{-1}$)	d_2
Uranium-235	5.2	0.12	2.4	0.011	1.1	0.14	2.5	0.011	1.1
Plutonium-239	5.4	0.14	2.9	0.011	1.1	0.15	3.0	0.011	1.1

as well as our fast-neutron data involving uranium-235 and plutonium-239. The study also required an estimation of the average preffission neutron energy we took from GEF. For that reason, we carried out a sensitivity study based on the worst combination of arbitrary $\pm 10\%$ error over these parameters. It proved the robustness of the separation between multichance fission channels from the $P(\nu)$ shapes and highlighted that the parameters associated with the standard deviation c_i and d_i are critical for the determination of precise second-chance ratio values. Hence, neutron-counting data for uranium-234 and plutonium-238 would improve our accuracy. Moreover, the method we have developed in this paper will be directly usable for the unfolding of such measurements.

The quite good agreement with GEF and ENDF-BVII *a posteriori* supports the main assumption we made: the linear relationship between incident neutron energy and standard deviation below the second-chance threshold seems to be preserved up to 12 MeV in the space of average excitation energy. This result is to be added to the recent observation of an approximately linear relationship between the average γ multiplicity and the average excitation energy beyond the multichance thresholds [42].

VI. CONCLUSION

This paper proposes a robust formalism based on the Tikhonov regularization to unfold the neutron-multiplicity distributions from the raw data of any neutron counter.

Since the Tikhonov regularization does not reduce the solution space of the unfolding problem to some simplistic functions but only regular ones, the unfolded neutron-multiplicity

distributions are more precise. The standard deviation is roughly linear with the incident neutron energy below the second-chance fission threshold with a slope of 0.011 ± 0.002 MeV $^{-1}$ for uranium-235 and 0.011 ± 0.003 MeV $^{-1}$ for plutonium-239. In addition, it exhibits a local minimum in the energy range of second-chance fission transition. A simple model based on a mixing ratio of the second- to first-chance channel highlights how this results from their competition to govern the shape of the neutron-multiplicity distributions. Assuming that the linearity is preserved in the space of average excitation energy, this competition was exploited to extract an indirect but first measurement of the second-chance partial probability.

The regularization procedure reaches its limits for dramatically poor statistics, which is why uranium-238 data were not operable. Furthermore, Fréhaut's data are affected by systematic errors larger than statistical errors. New measurements with a white neutron source could thus be valuable to reduce the uncertainties and generalize the study to higher-chance fissions. Such a program is being developed by CEA with the new detector SCONE [43] and the Neutrons For Science beam at GANIL [44].

APPENDIX: COMPLETE NEUTRON-MULTIPLICITY-DISTRIBUTION VALUES AND UNCERTAINTIES

The complete neutron-multiplicity distributions $P(\nu)$ unfolded by the regularization procedure are shown in Tables III–VI.

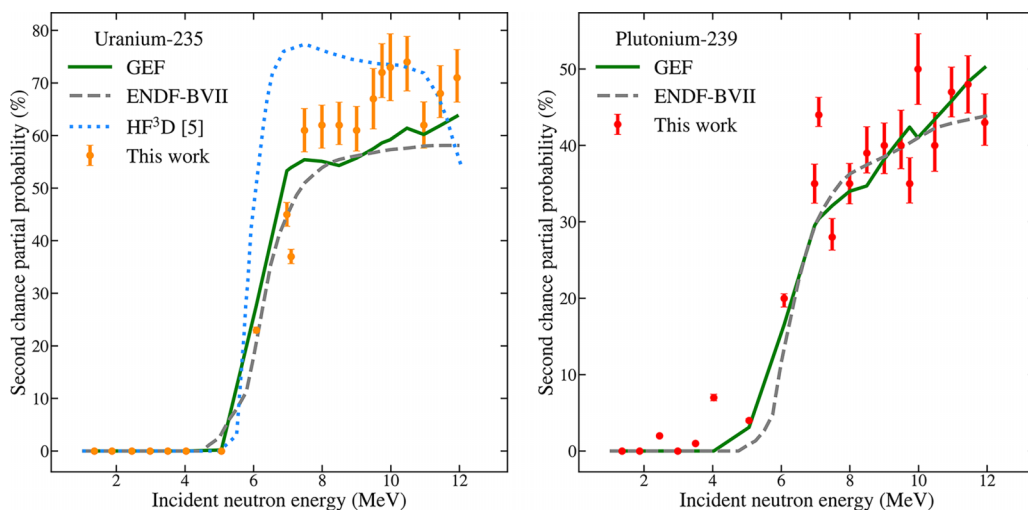


FIG. 6. Second-chance fission partial probability for uranium-235 (left) and plutonium-239 (right). The error bars include the statistical error propagation from Eq. (11) as well as arbitrary $\pm 10\%$ uncertainty over the average preffission neutron energy.

TABLE III. Complete neutron-multiplicity distributions for uranium-235 unfolded by the Tikhonov regularization procedure.

Neutron energy (MeV)	Regularization parameter	$p(0)$	$p(1)$	$p(2)$	$p(3)$	$p(4)$	$p(5)$	$p(6)$	$p(7)$	$p(8)$	$p(9)$
1.36	0.0000	0.0215	0.1618	0.3018	0.3233	0.1522	0.0385	0.0011	0.0000	0.0000	0.0000
1.87	0.0000	0.0192	0.1413	0.3098	0.3188	0.1656	0.0434	0.0020	0.0000	0.0000	0.0000
2.45	0.0000	0.0154	0.1318	0.2982	0.3238	0.1793	0.0457	0.0057	0.0001	0.0000	0.0000
2.98	0.0000	0.0135	0.1168	0.2958	0.3226	0.1919	0.0527	0.0067	0.0001	0.0000	0.0000
3.50	0.0000	0.0149	0.1003	0.2975	0.3234	0.1955	0.0664	0.0020	0.0000	0.0000	0.0000
4.03	0.0466	0.0098	0.0922	0.2851	0.3143	0.2231	0.0648	0.0078	0.0028	0.0002	0.0000
5.06	0.0000	0.0070	0.0767	0.2547	0.3312	0.2280	0.0953	0.0071	0.0000	0.0000	0.0000
6.08	0.0000	0.0050	0.0597	0.2011	0.3332	0.2626	0.1107	0.0276	0.0001	0.0000	0.0000
6.97	0.0178	0.0020	0.0319	0.1772	0.3302	0.2958	0.1298	0.0327	0.0004	0.0000	0.0000
7.09	0.0100	0.0024	0.0409	0.1739	0.3283	0.2777	0.1398	0.0369	0.0000	0.0000	0.0000
7.48	0.0214	0.0017	0.0289	0.1527	0.3217	0.3096	0.1448	0.0400	0.0008	0.0000	0.0000
7.99	0.0290	0.0013	0.0184	0.1628	0.2935	0.3273	0.1591	0.0369	0.0007	0.0000	0.0000
8.49	0.0317	0.0000	0.0239	0.1337	0.3069	0.3199	0.1640	0.0500	0.0016	0.0000	0.0000
9.00	0.0227	0.0016	0.0160	0.1282	0.2987	0.3176	0.1779	0.0592	0.0008	0.0000	0.0000
9.49	0.0322	0.0000	0.0121	0.1186	0.2840	0.3256	0.1981	0.0543	0.0057	0.0016	0.0000
9.74	0.0346	0.0000	0.0071	0.1132	0.2785	0.3285	0.2014	0.0697	0.0015	0.0000	0.0000
9.98	0.0440	0.0000	0.0119	0.1048	0.2686	0.3234	0.2128	0.0647	0.0103	0.0035	0.0000
10.47	0.0100	0.0011	0.0139	0.0925	0.2683	0.3259	0.2207	0.0775	0.0000	0.0000	0.0000
10.96	0.0713	0.0006	0.0064	0.0898	0.2665	0.3190	0.2058	0.0929	0.0190	0.0000	0.0000
11.44	0.0540	0.0005	0.0074	0.0903	0.2314	0.3310	0.2309	0.0791	0.0220	0.0075	0.0000
11.93	0.0735	0.0000	0.0070	0.0740	0.2376	0.3154	0.2422	0.0973	0.0213	0.0040	0.0011

TABLE IV. Statistical error propagated by Tikhonov regularization Eq. (11) for uranium-235. Notation: $p(i) \pm \Delta p(i)$.

Neutron energy (MeV)	Number of fissions	$\Delta p(0)$	$\Delta p(1)$	$\Delta p(2)$	$\Delta p(3)$	$\Delta p(4)$	$\Delta p(5)$	$\Delta p(6)$	$\Delta p(7)$	$\Delta p(8)$	$\Delta p(9)$
1.36	15538	0.0028	0.0036	0.0048	0.0067	0.0093	0.0128	0.0158	0.0196	0.0198	0.0118
1.87	15223	0.0028	0.0036	0.0048	0.0067	0.0093	0.0128	0.0158	0.0196	0.0198	0.0118
2.45	15263	0.0028	0.0036	0.0048	0.0067	0.0093	0.0128	0.0158	0.0196	0.0198	0.0118
2.98	18279	0.0028	0.0036	0.0048	0.0067	0.0093	0.0128	0.0158	0.0196	0.0198	0.0118
3.50	15225	0.0028	0.0036	0.0048	0.0067	0.0093	0.0128	0.0158	0.0196	0.0198	0.0118
4.03	22960	0.0028	0.0034	0.0043	0.0053	0.0062	0.0070	0.0067	0.0066	0.0061	0.0067
5.06	22874	0.0028	0.0036	0.0048	0.0067	0.0093	0.0128	0.0158	0.0196	0.0198	0.0118
6.08	10999	0.0028	0.0036	0.0048	0.0067	0.0093	0.0128	0.0158	0.0196	0.0198	0.0118
6.97	11376	0.0028	0.0036	0.0047	0.0064	0.0087	0.0112	0.0124	0.0140	0.0144	0.0099
7.09	20371	0.0028	0.0036	0.0048	0.0067	0.0093	0.0128	0.0158	0.0196	0.0198	0.0118
7.48	26486	0.0028	0.0035	0.0047	0.0063	0.0084	0.0107	0.0114	0.0124	0.0128	0.0094
7.99	23270	0.0028	0.0035	0.0046	0.0060	0.0077	0.0093	0.0093	0.0095	0.0097	0.0083
8.49	22734	0.0028	0.0035	0.0045	0.0059	0.0074	0.0088	0.0087	0.0087	0.0088	0.0079
9.00	25148	0.0028	0.0035	0.0047	0.0063	0.0082	0.0103	0.0108	0.0115	0.0119	0.0091
9.49	32735	0.0028	0.0035	0.0045	0.0059	0.0074	0.0088	0.0087	0.0087	0.0088	0.0079
9.74	23181	0.0028	0.0035	0.0045	0.0058	0.0072	0.0084	0.0082	0.0081	0.0081	0.0076
9.98	34456	0.0028	0.0034	0.0044	0.0054	0.0064	0.0073	0.0070	0.0069	0.0065	0.0069
10.47	23062	0.0028	0.0036	0.0048	0.0067	0.0093	0.0128	0.0158	0.0196	0.0198	0.0118
10.96	23251	0.0027	0.0032	0.0039	0.0045	0.0049	0.0052	0.0050	0.0052	0.0041	0.0055
11.44	22904	0.0027	0.0034	0.0042	0.0051	0.0058	0.0063	0.0060	0.0061	0.0053	0.0063
11.93	22376	0.0027	0.0032	0.0038	0.0044	0.0047	0.0051	0.0048	0.0051	0.0040	0.0054

TABLE V. Complete neutron-multiplicity distributions for plutonium-239 unfolded by the Tikhonov regularization procedure.

Neutron energy (MeV)	Regularization parameter	$p(0)$	$p(1)$	$p(2)$	$p(3)$	$p(4)$	$p(5)$	$p(6)$	$p(7)$	$p(8)$	$p(9)$
1.36	0.0000	0.0060	0.0763	0.2487	0.3231	0.2428	0.0882	0.0149	0.0000	0.0000	0.0000
1.87	0.0296	0.0054	0.0645	0.2390	0.3114	0.2658	0.0942	0.0198	0.0000	0.0000	0.0000
2.45	0.0331	0.0056	0.0567	0.2130	0.3275	0.2717	0.1005	0.0249	0.0000	0.0000	0.0000
2.98	0.0193	0.0051	0.0506	0.2016	0.3177	0.2701	0.1211	0.0338	0.0000	0.0000	0.0000
3.50	0.0342	0.0059	0.0420	0.1958	0.3067	0.2927	0.1249	0.0320	0.0000	0.0000	0.0000
4.03	0.0000	0.0030	0.0426	0.1556	0.3360	0.2825	0.1477	0.0327	0.0000	0.0000	0.0000
5.06	0.0000	0.0011	0.0271	0.1474	0.3089	0.2929	0.1705	0.0522	0.0000	0.0000	0.0000
6.08	0.0615	0.0011	0.0300	0.1090	0.2750	0.3400	0.1550	0.0800	0.0100	0.0000	0.0000
6.97	0.0426	0.0000	0.0137	0.1035	0.2366	0.3517	0.2107	0.0642	0.0190	0.0005	0.0000
7.09	0.0381	0.0015	0.0179	0.0916	0.2330	0.3415	0.2230	0.0617	0.0298	0.0000	0.0000
7.48	0.0208	0.0010	0.0120	0.0886	0.2490	0.3267	0.2231	0.0797	0.0199	0.0000	0.0000
7.99	0.0281	0.0000	0.0120	0.0749	0.2365	0.3403	0.2186	0.0978	0.0200	0.0000	0.0000
8.49	0.0424	0.0000	0.0070	0.0747	0.2072	0.3496	0.2181	0.1135	0.0299	0.0000	0.0000
9.00	0.0389	0.0000	0.0060	0.0670	0.2090	0.3130	0.2670	0.1080	0.0300	0.0000	0.0000
9.49	0.0187	0.0000	0.0080	0.0482	0.2108	0.3143	0.2661	0.1225	0.0301	0.0000	0.0000
9.74	0.0421	0.0000	0.0040	0.0517	0.2030	0.3085	0.2706	0.1224	0.0398	0.0000	0.0000
9.98	0.0389	0.0002	0.0040	0.0507	0.1821	0.3074	0.2984	0.1075	0.0497	0.0000	0.0000
10.47	0.0248	0.0000	0.0000	0.0555	0.1617	0.3211	0.2810	0.1313	0.0488	0.0007	0.0000
10.96	0.0206	0.0001	0.0060	0.0411	0.1675	0.2828	0.2978	0.1444	0.0602	0.0000	0.0000
11.44	0.0163	0.0000	0.0040	0.0359	0.1534	0.2948	0.2620	0.2002	0.0498	0.0000	0.0000
11.93	0.0226	0.0000	0.0000	0.0506	0.1168	0.3071	0.2767	0.1698	0.0766	0.0024	0.0000

TABLE VI. Statistical error propagated by Tikhonov regularization Eq. (11) for plutonium-239. Notation: $p(i) \pm \Delta p(i)$.

Neutron energy (MeV)	Number of fissions	$\Delta p(0)$	$\Delta p(1)$	$\Delta p(2)$	$\Delta p(3)$	$\Delta p(4)$	$\Delta p(5)$	$\Delta p(6)$	$\Delta p(7)$	$\Delta p(8)$	$\Delta p(9)$
1.36	22224	0.0028	0.0036	0.0049	0.0068	0.0095	0.0129	0.0158	0.0192	0.0193	0.0115
1.87	21724	0.0028	0.0035	0.0046	0.0061	0.0077	0.0092	0.0092	0.0090	0.0092	0.0079
2.45	21879	0.0028	0.0035	0.0046	0.0060	0.0074	0.0088	0.0086	0.0084	0.0084	0.0076
2.98	28017	0.0028	0.0036	0.0048	0.0065	0.0087	0.0112	0.0121	0.0132	0.0135	0.0095
3.50	22298	0.0028	0.0035	0.0046	0.0060	0.0073	0.0086	0.0085	0.0082	0.0082	0.0075
4.03	34044	0.0028	0.0036	0.0049	0.0068	0.0095	0.0129	0.0158	0.0192	0.0193	0.0115
5.06	33845	0.0028	0.0036	0.0049	0.0068	0.0095	0.0129	0.0158	0.0192	0.0193	0.0115
6.08	16106	0.0027	0.0033	0.0041	0.0049	0.0054	0.0058	0.0055	0.0056	0.0046	0.0058
6.97	14324	0.0028	0.0035	0.0044	0.0056	0.0066	0.0075	0.0072	0.0069	0.0065	0.0068
7.09	25349	0.0028	0.0035	0.0045	0.0058	0.0070	0.0081	0.0078	0.0075	0.0074	0.0072
7.48	27466	0.0028	0.0036	0.0048	0.0065	0.0085	0.0108	0.0115	0.0122	0.0125	0.0091
7.99	27436	0.0028	0.0035	0.0047	0.0062	0.0079	0.0096	0.0096	0.0096	0.0098	0.0082
8.49	23785	0.0028	0.0035	0.0044	0.0056	0.0067	0.0076	0.0073	0.0070	0.0067	0.0069
9.00	29643	0.0028	0.0035	0.0045	0.0058	0.0069	0.0080	0.0077	0.0074	0.0072	0.0071
9.49	31770	0.0028	0.0036	0.0048	0.0065	0.0087	0.0112	0.0121	0.0132	0.0135	0.0095
9.74	24759	0.0028	0.0035	0.0044	0.0056	0.0067	0.0076	0.0073	0.0070	0.0067	0.0069
9.98	38758	0.0027	0.0033	0.0040	0.0047	0.0051	0.0055	0.0052	0.0054	0.0043	0.0055
10.47	21618	0.0028	0.0035	0.0044	0.0056	0.0066	0.0075	0.0072	0.0069	0.0065	0.0068
10.96	30203	0.0027	0.0033	0.0040	0.0047	0.0051	0.0055	0.0052	0.0054	0.0043	0.0055
11.44	25788	0.0027	0.0031	0.0036	0.0041	0.0042	0.0045	0.0043	0.0046	0.0034	0.0048
11.93	28593	0.0027	0.0032	0.0039	0.0045	0.0048	0.0051	0.0048	0.0050	0.0039	0.0052

- [1] E. Dumonteil, R. Bahran, T. Cutler, B. Dechenaux, T. Grove, J. Hutchinson, G. McKenzie, A. McSpaden, W. Monange, M. Nelson, N. Thompson, and A. Zoia, *Commun. Phys.* **4**, 151 (2021).
- [2] O. A. Akindele, Ph.D. thesis, University of California, Berkeley, 2018.
- [3] J. Verbeke, *Nucl. Sci. Eng.* **182**, 481 (2016).
- [4] S. Okumura, T. Kawano, P. Jaffke, P. Talou, and S. Chiba, *Nucl. Sci. Tech.* **55**, 1009 (2018).
- [5] A. E. Lovell, T. Kawano, S. Okumura, I. Stetcu, M. R. Mumpower, and P. Talou, *Phys. Rev. C* **103**, 014615 (2021).
- [6] M. Soleilhac, J. Fréhaut, and J. Gauriau, *J. Nucl. Eng.* **23**, 257 (1969).
- [7] B. C. Diven, H. C. Martin, R. F. Taschek, and J. Terrell, *Phys. Rev.* **101**, 1012 (1956).
- [8] P. Santi and M. Miller, *Nucl. Sci. Eng.* **160**, 190 (2008).
- [9] M. Ribrag, J. Poitou, J. Matuszek, and C. Signarbieux, *Rev. Phys. Appl.* **7**, 197 (1972).
- [10] D. A. Hicks, J. Ise, and R. V. Pyle, *Phys. Rev.* **101**, 1016 (1956).
- [11] H. Condé and M. Holmberg, *Phys. Chem. Fission* **2**, 57 (1965).
- [12] J. W. Boldeman and A. W. Dalton, Technical Report No. AAEC/E-172, Australian Atomic Energy Commission Research Establishment, Lucas Heights, Australia, 1967, <https://www.osti.gov/biblio/4361627>.
- [13] D. S. Mather, P. Fieldhouse, and A. Moat, *Phys. Rev.* **133**, B1403 (1964).
- [14] J. C. Hopkins and B. C. Diven, *Nucl. Phys.* **48**, 433 (1963).
- [15] B. S. Holden and M. S. Zucker, *Nucl. Sci. Eng.* **98**, 174 (1988).
- [16] J. Fréhaut, Technical Report No. INDC(NDS)-220: 20083133, International Atomic Energy Agency (IAEA), Austria, 1988, https://inis.iaea.org/collection/NCLCollectionStore/_Public/20/083/20083133.pdf.
- [17] B. S. Wang, J. T. Harke, O. A. Akindele, R. J. Casperson, R. O. Hughes, J. D. Koglin, K. Kolos, E. B. Norman, S. Ota, and A. Saastamoinen, *Phys. Rev. C* **100**, 064609 (2019).
- [18] P. Marini, J. Taieb, D. Neudecker, G. Bélier, A. Chatillon, D. Etasse, B. Laurent, P. Morfouace, B. Morillon, M. Devlin, J. A. Gomez, R. C. Haight, K. J. Kelly, and J. M. O'Donnell, *Phys. Lett. B* **835**, 137513 (2022).
- [19] T. Ethvignot, M. Devlin, H. Duarte, T. Granier, R. C. Haight, B. Morillon, R. O. Nelson, J. M. O'Donnell, and D. Rochman, *Phys. Rev. Lett.* **94**, 052701 (2005).
- [20] A. Bzdak, R. Holzmann, and V. Koch, *Phys. Rev. C* **94**, 064907 (2016).
- [21] J. F. Wild, J. van Aarle, W. Westmeier, R. W. Loughheed, E. K. Hulet, K. J. Moody, R. J. Dougan, E.-A. Koop, R. E. Glaser, R. Brandt, and P. Patzelt, *Phys. Rev. C* **41**, 640 (1990).
- [22] A. Veyssiere, H. Beil, R. Bergere, P. Carlos, A. Lepretre, and K. Kernbath, *Nucl. Rev. A* **199**, 45 (1973).
- [23] O. Akindele, R. Casperson, B. Wang, J. Harke, R. Hughes, S. Fisher, A. Saastamoinen, and E. Norman, *Nucl. Instrum. Methods Phys. Res., Sect. A* **872**, 112 (2017).
- [24] J. Fréhaut, Technical Report No. INDC(NDS)-220: 20082950, International Atomic Energy Agency (IAEA), Austria, 1989, https://inis.iaea.org/collection/NCLCollectionStore/_Public/20/082/20082950.pdf.
- [25] J. P. Lestone, [arXiv:1409.5346](https://arxiv.org/abs/1409.5346).
- [26] J. Hadamard, Lecture delivered at Yale University, 1923.
- [27] L. Tenorio, *SIAM Rev.* **43**, 347 (2001).
- [28] M. S. Zucker and N. E. Holden, Technical Report No. CONF-850610, Brookhaven National Lab., Upton, NY, 1985, <https://www.osti.gov/biblio/5042461>.
- [29] M. S. Zucker and N. E. Holden, Technical Report No. BNL-48109, Brookhaven National Lab., Upton, NY, 1992, <https://www.osti.gov/servlets/purl/10117903>.
- [30] M. Dakowski, Y. A. Lazarev, V. F. Turchin, and L. S. Turovtseva, *Nucl. Instr. Meth. A* **113**, 195 (1973).
- [31] R. S. Mukhin, *Phys. Part. Nucl. Lett.* **18**, 439 (2021).
- [32] A. V. Isaev, R. S. Mukhin, A. V. Andreev, M. A. Bychkov, M. L. Chelnokov, V. I. Chepigin, H. M. Devaraja, O. Dorvaux, M. Forge, B. Gall, K. Hauschild, I. N. Izosimov, K. Kessaci, A. A. Kuznetsova, A. Lopez-Martens, O. N. Malyshev, A. G. Popeko, Y. A. Popov, A. Rahmatinejad, B. Sailaubekov *et al.*, *Eur. Phys. J. A* **58**, 108 (2022).
- [33] E. H. Moore, *Bull. Amer. Math. Soc.* **26**, 394 (1920).
- [34] R. Penrose, *Math. Proc. Camb. Phil. Soc.* **51**, 406 (1955).
- [35] Z. Bai and J. W. Demmel, Technical Report No. UCB/CSD-92-720, EECS Department, University of California, Berkeley, 1992, <http://www2.eecs.berkeley.edu/Pubs/TechRpts/1992/6016.html>.
- [36] R. Aster, B. Borchers, and C. H. Thurber, *Parameter Estimation and Inverse Problems* (Elsevier, Amsterdam, 2005).
- [37] P. C. Hansen, *Numer. Algor.* **6**, 1 (1994).
- [38] J. Terrell, *Phys. Chem. Fission* **2**, 3 (1965).
- [39] R. L. Henkel, *Monographs and Texts in Physics and Astronomy* **4**, 2001 (1963).
- [40] K.-H. Schmidt, B. Jurado, C. Amouroux, and C. Schmitt, *Nucl. Data Sheets* **131**, 107 (2016).
- [41] <https://t2.lanl.gov/nis/data/astro/molnix96/sepn.html>.
- [42] N. P. Giha, S. Marin, J. A. Baker, I. E. Hernandez, K. J. Kelly, M. Devlin, J. M. O'Donnell, R. Vogt, J. Randrup, P. Talou, I. Stetcu, A. E. Lovell, O. Litaize, O. Serot, A. Chebboubi, C. Y. Wu, S. D. Clarke, and S. A. Pozzi, *Phys. Rev. C* **107**, 014612 (2023).
- [43] G. Bélier, B. Fraïsse, A. Francheteau, L. Gaudefroy, V. Méot, and O. Roig, *Nucl. Instrum. Methods Phys. Res. A* (to be published).
- [44] X. Ledoux, J.-C. Foy, J.-E. Ducret, A.-M. Frelin, D. Ramos, J. Mrazek, E. Simeckova, R. Behal, L. Caceres, V. Glagolev, B. Jacquot, A. Lemasson, J. Pancin, J. Piot, C. Stodel, and M. Vandebrouck, *Eur. Phys. J. A* **57**, 257 (2021).